

# Mesons, baryons and waves in the baby Skyrmion model

A. Kudryavtsev<sup>1</sup>, B. Piette, W.J. Zakrzewski
 Department of Mathematical Sciences, University of Durham, Durham DH1 3LE, England  
 (e-mail: Kudryavtsev@vitep5.itep.ru, B.M.A.G.Piette@uk.ac.durham, W.J.Zakrzewski@uk.ac.durham)

Received: 6 February 1997

**Abstract.** We study various classical solutions of the baby-Skyrmion model in  $(2+1)$  dimensions. We point out the existence of higher energy states, interpret them as resonances of Skyrmions and anti-Skyrmions and study their decays. Most of the discussion involves a highly excited Skyrmion-like state with winding number one which decays into an ordinary Skyrmion and a Skyrmion-anti-Skyrmion pair. We also study wave-like solutions of the model and show that some of such solutions can be constructed from the solutions of the sine-Gordon equation. We also show that the baby-Skyrmion model has non-topological stationary solutions. We study their interactions with Skyrmions.

## 1 Introduction

In previous papers by two of us (BP and WJZ) [1–3] some hedgehog-like solutions of the so called baby-Skyrmion model were studied. It was shown there that the model has soliton-like topologically stable static solutions (called baby-Skyrmions) and that these solitons can form bound states. The interaction between the solitons was studied in detail and it was shown that the long distance force between 2 baby-Skyrmions depends on their relative orientation.

To construct these soliton solutions, one must use a radially symmetric ansatz (hedgehog configuration) and reduce the equation for the soliton to an ordinary differential equation. This equation admits more solutions than those described in [2] and [3] and, as we will show, they correspond to excited states or resonances made out of both Skyrmions and anti-Skyrmions. We will also show that the model admits some solutions in the form of non-linear waves.

The  $(2+1)$ -dimensional baby-Skyrmion field theory model is described by the Lagrangian density

$$L = F_\pi \left( \frac{1}{2} \partial_\alpha \phi \partial^\alpha \phi - \frac{k^2}{4} (\partial_\alpha \phi \times \partial_\beta \phi) (\partial^\alpha \phi \times \partial^\beta \phi) - \mu^2 (1 - \mathbf{n} \cdot \phi) \right). \quad (1)$$

Here  $\phi \equiv (\phi_1, \phi_2, \phi_3)$  denotes a triplet of scalar real fields which satisfy the constraint  $\phi^2 = 1$ ;  $(\partial_\alpha \partial^\alpha = \partial_t \partial^t - \partial_i \partial^i)$ . As mentioned in [1–3] the first term in (1) is the familiar Lagrangian density of the pure  $S^2$   $\sigma$  model. The second term, fourth order in derivatives, is the  $(2+1)$  di-

mensional analogue of the Skyrme-term of the three-dimensional Skyrme-model [4]. The last term is often referred to as a potential term. The last two terms in the Lagrangian (1) are added to guarantee the stability of a Skyrmion [5].

The vector  $\mathbf{n} = (0, 0, 1)$  and hence the potential term violates the  $O(3)$ -rotational iso-invariance of the theory. The state  $\phi_3 \equiv 1$  is the vacuum state of the theory. As in [1, 2] we fix our units of energy and length by setting  $F_\pi = k = 1$  and choose  $\mu^2 = 0.1$  for our numerical calculations. The choice  $\mu^2 = 0.1$  sets the scale of the energy distribution for a basic Skyrmion.

As usual we are interested mainly in field configurations for which the potential energy at infinity vanishes as only they can describe field configurations with finite total energy. Therefore we look for solutions of the equation of motion for the field  $\phi$  which satisfies

$$\lim_{|x| \rightarrow \infty} \phi(\mathbf{x}, t) = \mathbf{n} \quad (2)$$

for all  $t$ . This condition formally compactifies the physical space to a 2-sphere  $S_{ph}^2$  and so all maps from  $S_{ph}^2$  to  $S_{iso}^2$  are characterised by the integer-valued degree of this map (the topological charge).

The analytical formula for this degree is

$$deg[\phi] = \frac{1}{4\pi} \int \phi \cdot (\partial_1 \phi \times \partial_2 \phi) d^2 x. \quad (3)$$

This degree is a homotopy invariant of the field  $\phi$  and so it is conserved during the time evolution.

The Euler-Lagrange equation for the Lagrangian  $L$  (1) is

$$\partial^\alpha (\phi \times \partial_\alpha \phi - \partial_\beta \phi (\partial^\beta \phi \cdot \phi \times \partial_\alpha \phi)) = \mu^2 \phi \times \mathbf{n}. \quad (4)$$

One simple solution of (4) is given by  $\phi(\mathbf{x}, t) = \mathbf{n}$ . This solution is of degree zero and describes the vacuum

---

<sup>1</sup> also at ITEP, Moscow, Russia

configuration. Another simple solution of (1.4) is evidently  $\phi = -\mathbf{n}$ . It is also of degree zero and may be considered as a false vacuum configuration.

## 2 Static Skyrme solutions

Some static solutions of the equation of motion (3) were discussed in [1,2]. An important class of static solutions of the equation of motion consists of fields which are invariant under the group of simultaneous spatial rotations by an angle  $\alpha \in [0, 2\pi]$  and iso-rotations by  $-\alpha$ , where  $n$  is a non-zero integer. Such fields are of the form

$$\phi(\mathbf{x}) = \begin{pmatrix} \sin f(r) \cos(n\theta) \\ \sin f(r) \sin(n\theta) \\ \cos f(r) \end{pmatrix}, \quad (5)$$

where  $(r, \theta)$  are polar coordinates in the  $(x, y)$ -plane and  $f$  is a function which satisfies certain boundary conditions which will be specified below. Such fields are analogues of the hedgehog field of the Skyrme model and were studied in [3] for different values of  $\mu^2$ .

The function  $f(r)$ , the analogue of the profile function of the Skyrme model, has to satisfy

$$f(0) = m\pi, m \in Z \quad (6)$$

for the field (5) to be regular at the origin. To satisfy the boundary condition (2) we set

$$\lim_{r \rightarrow \infty} f(r) = 0. \quad (7)$$

Then solutions of the equation of motion which satisfy (6) and (7) describe fields for which the total energy is finite. Moreover, the degree of the fields (5) is

$$\text{deg}[\phi] = [\cos f(\infty) - \cos f(0)] \frac{n}{2}. \quad (8)$$

For fields which satisfy the boundary conditions (6) and (7) and which thus correspond to finite energy configurations, we get from (8)

$$\text{deg}[\phi] = [1 - (-1)^m] \frac{n}{2}. \quad (9)$$

The fields of the form (5) which are stationary points of the static energy functional  $V$ , the time independent part of  $L$  in (1), must satisfy the Euler-Lagrange equation for  $f$

$$\begin{aligned} & \left( r + \frac{n^2 \sin^2 f}{r} \right) f'' \\ & + \left( 1 - \frac{n^2 \sin^2 f}{r^2} + \frac{n^2 f' \sin f \cos f}{r} \right) f' \\ & - \frac{n^2 \sin f \cos f}{r} - r\mu^2 \sin f = 0. \end{aligned} \quad (10)$$

In [1, 2] it was shown that the solutions of (10) for  $n = 1, 2$  and  $m = 1$ , correspond to the absolute minima of the energy functional of degree 1 and 2 respectively.

Any field obtained by translating and iso-rotating the solution corresponding to  $n = m = 1$  was called a baby Skyrme. As this field configuration has a topological charge  $\text{deg}[\phi] = 1$  we call it a ‘‘baryon’’ and denote it by the symbol  $B$ . A solution corresponding to  $n = -1$  and  $m = 1$  is then an anti-Skyrmion or an antibaryon  $\bar{B}$ .

Clearly, there exist also solutions of the equation of motion which satisfy the boundary conditions (6) at the origin but which, at infinity, behave as

$$\begin{aligned} \lim_{r \rightarrow \infty} f(r) &= l\pi. \\ l &\in Z. \end{aligned} \quad (11)$$

Such fields, if  $l$  is odd, differ from  $B$ -Skyrmions in that they describe solutions with finite energies. As we are interested in fields of finite energy, in this paper, we restrict our attention to  $B$ -Skyrmions.

It is worth mentioning that the asymptotic behaviour of  $B$ -Skyrmions is given by [2]:

$$f(r) \sim K_n(\mu r) \sim_{r \rightarrow \infty} \sqrt{\frac{1}{2\pi\mu r}} e^{-\mu r} \quad (12)$$

where  $K_n(x)$  is the modified Bessel function.

We have solved (10) for different values of  $n$  and  $m$  using a shooting method with the appropriate boundary condition (6, 7). We have determined the profile function  $f(r)$  and the energy and topological density profiles for each of these solutions.

In Fig. 1, we show the profile functions  $f(r)$  for different values of  $n$  and  $m$ .

The total energies for our solutions are as follows:

$n \setminus m$	1	2	3	4
1	1.5642	5.011	10.030	16.492
2	2.9359	7.725	14.185	22.233
3	4.4698	10.555	18.350	27.819
4	6.1145	13.465	22.633	33.395

When  $m = 1$ , the topological charge is given by  $n$ , and each configuration is a superposition of  $n$  Skyrmions. We know from [2] that only the first two are stable. Figure 2 shows the profiles of the energy and of the topological density of the states  $n = 1$  and  $n = 2$ .

When  $m = 2$ , the topological charge is 0 and, as can be seen from Fig. 3, these configurations correspond to a superposition of  $n$  Skyrmions and  $n$  anti-Skyrmions where the Skyrmions form a ring surrounding the anti-Skyrmion at the centre. We have integrated separately both the positive and negative parts of the topological charge, and have found them to be  $n$  and  $-n$  respectively, thus justifying our interpretation.

When  $m = 3$ , the topological charge is given by  $n$ , and each configuration is a superposition of  $2n$  Skyrmions and  $n$  anti-Skyrmions (Fig. 4). The configuration is made of 3 layers, with  $n$  Skyrmions at the centre,  $n$  anti-Skyrmions in the middle, and  $n$  Skyrmions in the outside ring.

Note that when  $m$  is larger than 1 the energy of the configuration is larger than the energy of  $nm$  baby Skyrmions. This indicates that such configurations are unstable and we will now analyse their decay modes.

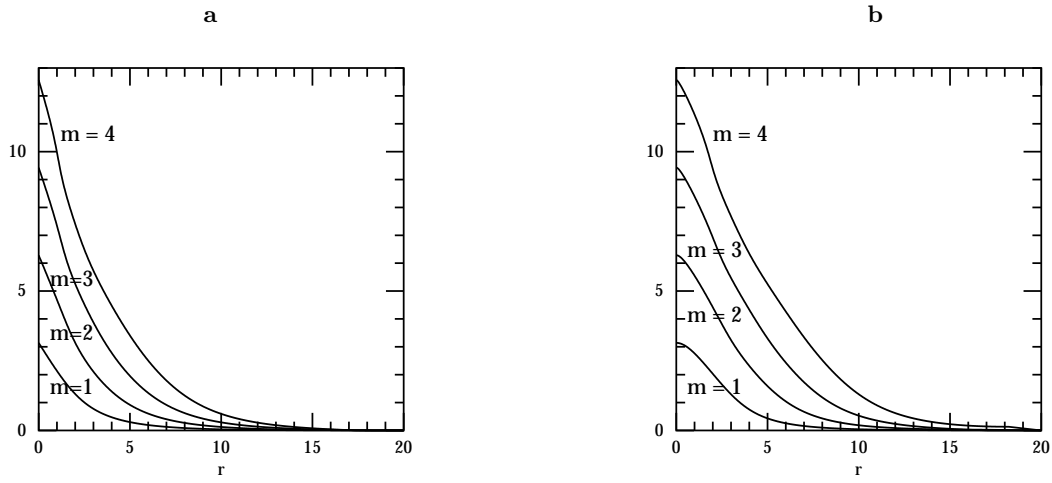


**Fig. 1. a:** Profiles for the hedgehog solutions:  $n = 1, m = 1, 2, 3, 4$  **b:** Profiles for the hedgehog solutions:  $n = 2, m = 1, 2, 3, 4$

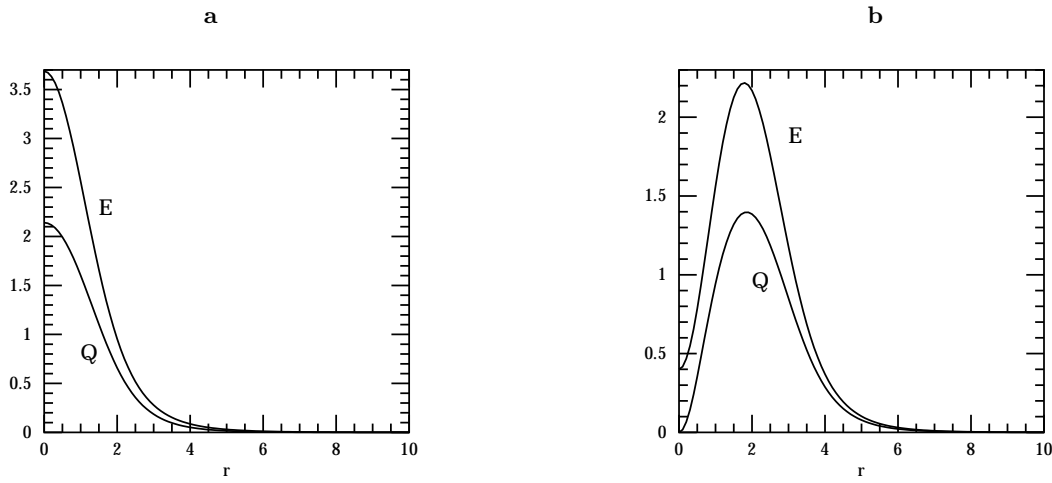


**Fig. 2. a:** Energy and topological charge density for the hedgehog solution:  $n = 1, m = 1$  **b:** Energy and topological charge density for the hedgehog solution:  $n = 2, m = 1$

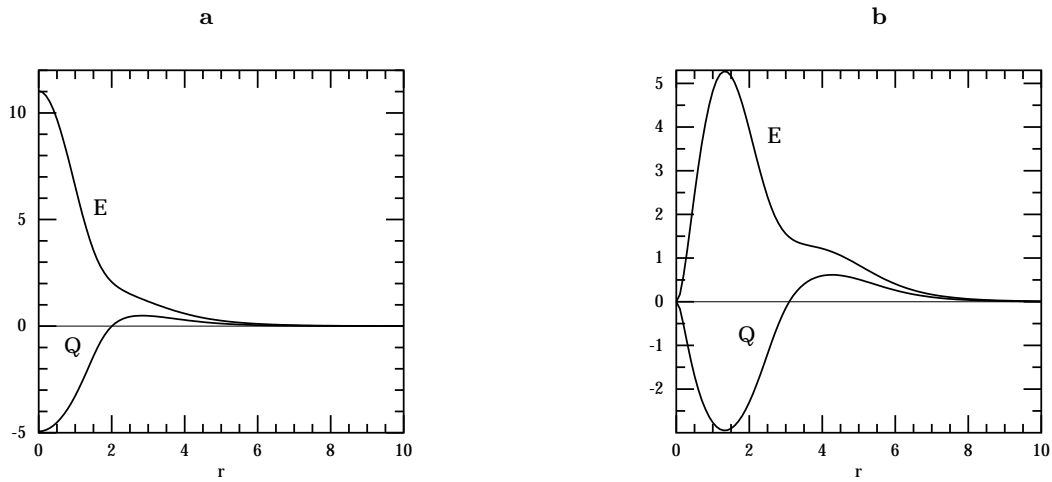


**Fig. 3. a:** Energy and topological charge density for the hedgehog solution:  $n = 1, m = 2$  **b:** Energy and topological charge density for the hedgehog solution:  $n = 2, m = 2$

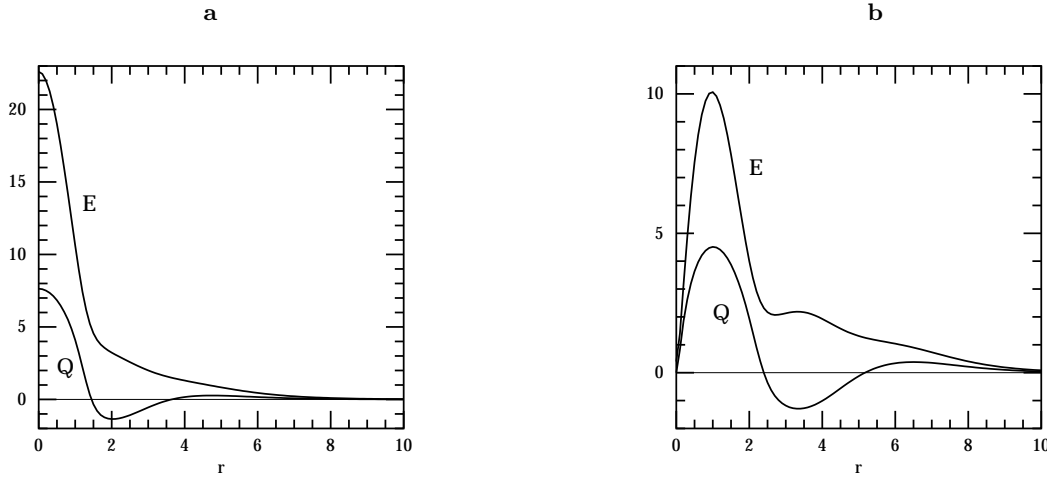


**Fig. 4. a:** Energy and topological charge density for the hedgehog solution:  $n = 1, m = 3$  **b:** Energy and topological charge density for the hedgehog solution:  $n = 2, m = 3$

### 3 Exited meson $M_{1,2}(n = 1; m = 2)$

Let us look first at the field which corresponds to  $n = 1, m = 2$ . From (8) we see that the topological charge of this field configuration is zero. So we can call this state, a “meson” or a coherent “meson cloud”. We note from Fig. 3a that, like a  $B$  Skyrmion, this solution corresponds to a radially symmetric extended configuration with the maximum of the energy density at the origin ( $r = 0$ ).

As the total energy (5.011) exceeds the sum of the masses of a  $B$ -Skyrmion and a  $\bar{B}$ -Skyrmion ( $2 \times 1.5642$ ), this configuration is unstable.

The distribution of the topological charge density shows more structure (Fig. 3a). We note that the topological charge density is negative for small  $r$  and that it changes sign at  $r = r_{cr} = 2$ . At this point the profile function  $f(r_{cr}) = \pi$ , thus the solution corresponding to the  $M_{1,2}$  state looks like a Skyrmion surrounded by an anti-Skyrmion field. Of course the total topological charge is zero. We see that the solution still looks like an extended but localised configuration. However, although the topological charge density suggests that the Skyrmion is at the origin the profile function there is given by  $f = 2\pi$  and so, from this point of view, resembles more the vacuum than a Skyrmion. This suggests a possible interpretation of the  $M_{1,2}$  state in terms of Skyrmons and anti-Skyrmions. Whatever the interpretation, the state is mesonic in nature. Moreover, looking at the field configuration we note that most of its changes takes place around those points in the  $(x, y)$  plane where  $r = r_{cr}$  *i.e.* where  $f = \pi$ . It is remarkable that everywhere along this circle  $\phi_3 = -1$ . This circle is actually the region of instability when the solution  $M_{1,2}$  is excited by a non-radial perturbation of small amplitude.

In fact, it is not difficult to demonstrate that at each point on the circle  $r = r_{cr}$  one can create “hedgehog-like” extended objects using only infinitesimal perturbations. Of course, if these extended objects were to correspond to Skyrmons and anti-Skyrmions then to conserve the topo-

logical charge they will have to be created in pairs and we would expect them to appear as soon as we perturb the initial configuration. To check for such a behaviour we have perturbed the initial configuration corresponding to the  $M_{1,2}$ -state. Our perturbation was in the form of small excess of kinetic energy centered around two points in the  $(x, y)$ -plane chosen symmetrically with respect to  $r = 0$ . We have found that, indeed, the state split into a Skyrmion and anti-Skyrmion pair of the  $B$ -type. Their relative orientation was such that the force between them was repulsive. After their creation the Skyrmion and the anti-Skyrmion moved in opposite directions from the centre.

We then experimented with distorting the initial state by different perturbations and we observed different decay modes. When the applied perturbation was not symmetric with respect to  $r = 0$  (but was close to being symmetric) the  $M_{1,2}$  state decayed into a Skyrmion and an anti-Skyrmion, which then rotated in their internal space so that their relative orientation made them to attract each other. They then collided into each other and decayed into waves.

We thus conclude that the solution  $M_{1,2}$  of (10) is indeed a saddle point in the space of field configurations. The state can be thought of as a resonance of a Skyrmion and an anti-Skyrmion and it has different decay modes when perturbed. It decays either into a  $B\bar{B}$ -pair or into light “mesons”.

It would be interesting to see whether it is possible to create the  $M_{1,2}$  state in a head-on collision of a Skyrmion and an anti-Skyrmion. We are planning to come back to this question in a future paper.

### 4 Exited $B_{1,3}$ baryon ( $n = 1, m = 3$ )

This is a baryon-type state as its topological charge is one. The profiles of the energy and of the topological charge densities for this state are shown in Fig. 4a. Looking at

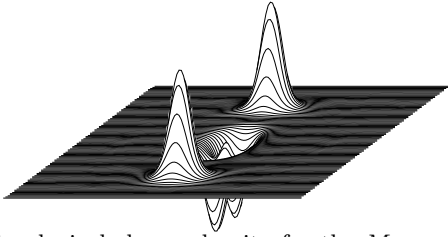


**Fig. 5.** Topological charge density for the  $M_{2,2} \rightarrow B + \bar{B} + B + \bar{B}$  decay mode

the density of the topological charge we see that this state may be considered as the usual  $B$ -Skyrmion surrounded by an anti-Skyrmion and a further Skyrme ring. The configuration has an energy larger than the energy of its constituents and is thus unstable.

We have performed several simulations looking at the decay products of this state. When we used a perturbation symmetric with respect to the origin the configuration decayed into 2 Skyrmeons and 1 anti-Skyrmion, the anti-Skyrmion staying at the origin, while the two Skyrmeons moved in opposite directions. When the perturbation was not symmetric, the Skyrmeons and the anti-Skyrmion were able to change their relative orientations and one of the Skyrmeons collided with the anti-Skyrmion and decayed into waves.

## 5 Mesons made from dibaryons and anti-dibaryons

Let us now discuss various properties and decay modes of excited meson-like states made out of dibaryons (a bound state of 2  $B$ -Skyrmions) and antidibaryons. We will concentrate our attention on the  $n = 2$  and  $m = 2$  state but our discussion generalises easily to other states. The topological charge of the  $(n = 2, m = 2)$  configuration (i.e. its baryon number) is zero, so this configuration is a meson-like state from the point of view of our classification. As  $n = 2$  the configuration looks like a dibaryon near the origin, i.e. near  $r = 0$ . From Fig. 3b, we see that it corresponds to a dibaryon at the origin surrounded by an anti-dibaryon ring. The border between these two regions of opposite topological charge is, again, very well defined and is situated along the circle of radius  $r_{cr} = 3$ , ( $f(r_{cr}) = \pi$ ). So this ring is again the region of instability. Applying different types of perturbations to our  $(n = 2, m = 2)$  solution, we have observed three different decay modes for this state:

$$M_{2,2} \rightarrow \begin{cases} B + \bar{B} + B + \bar{B} \\ B + \bar{B} + \text{waves} \\ \text{waves} \end{cases} . \quad (13)$$

The picture of the energy density for the first decay modes is shown in Fig. 5.

## 6 Other excited mesonic and baryonic states

- i) Let us look first at the state  $(n = 1, m = 4)$ . This state, again, is mesonic with  $\text{deg}[\phi] = 0$ . The energy and topological charge profiles are shown in Fig. 6. The state is more complicated as its energy density exhibits additional maxima and minima. In fact, the state looks as if it were a coherent state of Skyrmeons and anti-Skyrmions, with rings of different radii occupied by fields of alternating topological charge. This is clearly seen from the topological charge density plots; moreover, the total topological charge in each ring is  $+1, -1, +1$  and  $-1$  respectively (going out from  $r = 0$ ). Thus we denote this state as  $M_{1,4}$  meson.
- ii) Another interesting state is that of  $M_{2,3}$  ( $n = 2, m = 3$ ). Its topological charge is 2. Hence this state can be thought of as an excited state of the dibaryon  $M_{2,1}$ . Its energy is clearly quite large and the state represents a coherent mixture of 4 Skyrmeons and 2 anti-Skyrmions and so it can decay into different channels. One example of its decay mode is shown in Fig. 7. We see in this picture that the decay products consist of two outgoing Skyrmeons and two anti-Skyrmions with the remaining 2 Skyrmeons at rest close to the origin. The fact that the decay products involve one di-Skyrmion at the origin (slightly excited) is due to the attraction between two Skyrmeons, as  $\text{mass}(M_{2,1}) < 2 \text{mass}(B)$ , see our table in Sect. 2.
- iii) Another interesting state is  $M_{2,4}$  which corresponds to  $(n = 2, m = 4)$  and, as such, is a highly excited meson state. Its energy and topological charge profiles are shown in Fig. 6b.

Clearly, the list of new solutions may be continued further by taking larger values of  $n$  and  $m$ . Of course, having calculated some of their profile functions we see that as one increases  $m$  their energies increase (quite rapidly). All these higher energy states can be treated as coherent states of some number of Skyrmeons and anti-Skyrmions and are unstable. Under suitable perturbations they will decay into various channels involving Skyrmeons and anti-Skyrmions with some Skyrmeons and anti-Skyrmions annihilating into pure waves.

## 7 Plane wave solutions

Let us now look at wave-like solutions of our model. Recall that such wave-like solutions have already been studied in [6, 7] for a slightly different version of a “skyrme-like” (2+1) dimensional model (the potential term of that model was different.)

What type of waves can we find for the Lagrangian in the form (1)? To look for plane wave-like solutions, we seek solutions which do not depend on one variable, say  $y$ . However, as soon as we impose this condition we note that the Skyrme-like term vanishes for these field configurations. So the discussion is not that difficult and can be performed analytically.

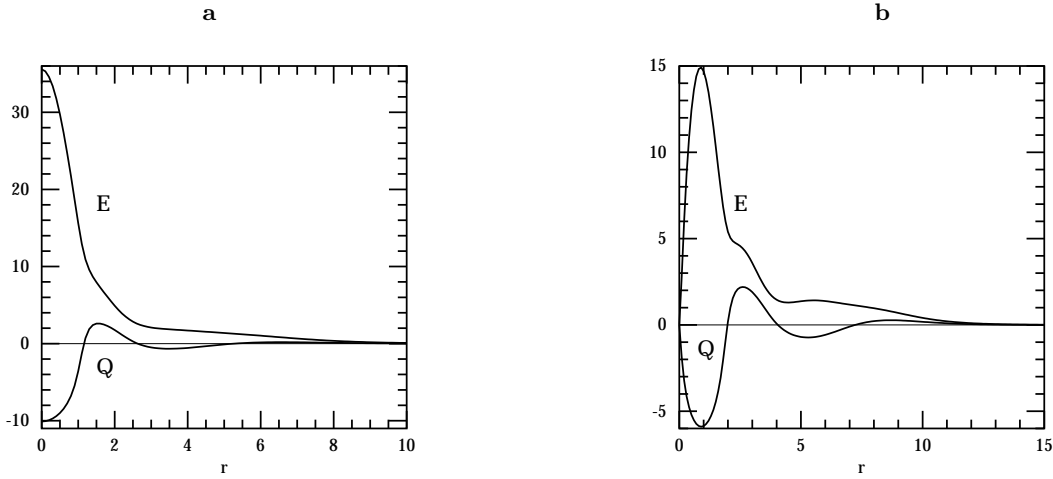


**Fig. 6. a:** Energy and Topological charge density for the hedgehog solution:  $n = 1, m = 4$  **b:** Energy and Topological charge density for the hedgehog solution:  $n = 2, m = 4$

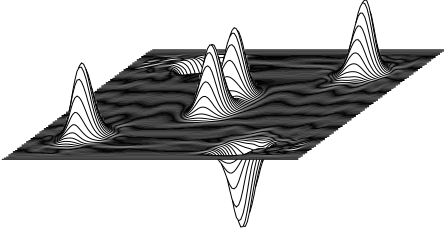


**Fig. 7.** Topological charge density for the  $M_{2,3} \rightarrow B + \bar{B} + B + \bar{B} + B + B$  decay mode

First, we look for solutions of the equation of motion for the field  $\phi$  in the form:

$$\phi = (\sin f \cos \psi, \sin f \sin \psi, \cos f), \quad (14)$$

where  $f = f(x, t)$  and  $\psi = \psi(x, t)$ . In terms of  $f$  and  $\psi$  the Lagrangian takes the form

$$L = (1/2) \int d^2x \left( \partial_\mu f \partial^\mu f + ((1 - \cos(2f))/2) \partial_\mu \psi \partial^\mu \psi - \mu^2 (1 - \cos(f)) \right). \quad (15)$$

To go further we consider the case when the phase  $\psi$  is constant. In this case the field  $f$  satisfies

$$\partial_\mu \partial^\mu f + \mu^2 \sin(f) = 0, \quad (16)$$

which is the sine-Gordon equation. So we see that when  $\psi = \text{const}$  the wave solutions of the Lagrangian (1) are given by the solutions of the sine-Gordon equation.

Moreover, solutions of (16) with small amplitude may be considered as ordinary plane waves with the dispersion relation given by

$$\omega^2 = \mu^2 + k^2. \quad (17)$$

Of all finite energy solutions of (16) (one-dimensional case) the most important, and perhaps the best studied, is the solution of the kink type:

$$f(x, t) = 4 \operatorname{atan} \left( \exp \left[ -\mu \left( \frac{x - x_0 - vt}{\sqrt{1 - v^2}} \right) \right] \right). \quad (18)$$

When translated to our case we note that when  $x$  changes from  $-\infty$  to  $+\infty$ , the vector  $\phi$  moves along the meridional cross-section of the  $S^2_{iso}$ -sphere and returns to the same point. Moreover, this is true for any fixed time  $t$ .

Another solution of (16), called breather, is also well known and has been studied by many people. Its form is [8]

$$f(x, t) = 4 \operatorname{atan} \left( \frac{(1 - \omega^2)^{1/2}}{\omega} \frac{\sin(\omega(t - t_0))}{\cosh((1 - \omega^2)^{1/2}(x - x_0))} \right) \quad (19)$$

where  $\omega$  is the frequency of the internal breather oscillations.

These 2 types of solitonic waves are infinite front lines (the solutions depend only on one spatial variable,  $x$ ). Unfortunately, once imbedded into  $S^2$ , the target space for our model, the extra degrees of freedom make these waves unstable. For the kink solution this is not surprising as the “loop” around the meridian can easily “slip” on one side of the sphere, thus decreasing the potential energy.

To see this, let us take the configuration

$$\phi(\mathbf{x}) = \begin{pmatrix} \cos \alpha \sin f \\ \sin \alpha \cos \alpha (1 - \cos f) \\ 1 - \cos^2 \alpha (1 - \cos f) \end{pmatrix}, \quad (20)$$

where  $f$  is given by (18) with  $v$  set to 0, and where  $\alpha$  is a function which depends only on  $y$  and which goes to 0 when  $y$  goes to infinity. This configuration describes the kink (18, 14) perturbed locally in  $x$  and  $y$ , and it “displaces” the kink from the meridian of the 2-sphere onto a loop of a smaller radius on  $S^2$ . The energy density for this static configuration is given by

$$E = \int dx dy \left[ \frac{1}{2} [\cos^2 \alpha f_x^2 + \alpha_y^2 (\sin^2 \alpha \sin^2 f + (1 - \cos f)^2) + k^2 f_x^2 \alpha_y^2 (1 - \cos f)^2 \cos^2 \alpha] + \mu^2 \cos^2 \alpha (1 - \cos f) \right]. \quad (21)$$

To prove that for some appropriate choice of  $\alpha$ , the energy decreases, we compute the change of energy induced by a non-zero  $\alpha$

$$\begin{aligned} \delta E &= E(\alpha = 0) - E(\alpha) \\ &= \int dx dy \left[ 2 \sin^2 \frac{f}{2} \left[ \mu^2 (\sin^2 \alpha - k^2 \alpha_y^2 (1 - \cos f)^2 \cos \alpha) \right. \right. \\ &\quad \left. \left. - \alpha_y^2 (1 + \sin^2 \alpha \cos \frac{f}{2}) \right] + \mu^2 \sin^2 \alpha (1 - \cos f) \right] \\ &\geq \int dx dy \left[ 2 \sin^2 \frac{f}{2} \left[ \mu^2 (\sin^2 \alpha - k^2 \alpha_y^2 \cos \alpha) \right. \right. \\ &\quad \left. \left. - \alpha_y^2 (1 + \sin^2 \alpha) \right] + \mu^2 \sin^2 \alpha (1 - \cos f) \right] \end{aligned} \quad (22)$$

where we have used the fact that for (18)  $f_x = 2\mu \sin(f/2)$ . Given  $\alpha(y)$  satisfying the asymptotic behaviour imposed, we can always stretch it by performing the dilation  $y \rightarrow ay$  to make  $\alpha_y$  small enough to make the two negative terms in (22) smaller than the positive terms. This proves the instability of the sine-Gordon kink wave when imbedded into the  $S^2$  model.

We have performed some numerical simulations for both types of waves and have indeed observed their instability. In both cases, as soon as some region of the wave is perturbed, the wave collapses around this point, emitting radiation. The collapse front then propagates rapidly along the solitonic wave destroying it completely.

In our previous work [7], we have studied the scattering properties of plane waves and Skyrmions. The Skyrmions studied in [7] were different (the potential was different) so we have repeated our analysis for the model studied here and have found no major difference. Like in the previous case, the Skyrmion absorbs a section of the wave and starts moving after the collision.

We have also studied the scattering between a Skyrmion and the sine-Gordon front waves. We observed that when the Skyrmion is close to a sine-Gordon wave (breather or kink) it triggers the wave collapse and, as a result, there is no real scattering between these two objects.

While performing simulations with large amplitude breather waves we have observed the formation of a radially symmetric breather-like soliton. This solution looks very similar to the pulsions observed in [9]. We discuss some of its properties in the next section.

## 8 Non-topological Solitons

In the previous section we have described our studies of waves in the baby-Skyrmion model in which we observed that the plane wave solutions which are given by the solutions of the (1+1) dimensional sine-Gordon equation are unstable.

However, when we looked at the decay of some breather front waves we encountered something rather unexpected. Instead of decaying into waves that dissipate like kink solutions they produced a radially symmetric breather-like field configuration which appeared to be relatively stable. By looking at the time evolution of this field

configuration, as produced by our simulation, we were able to conclude that:

- the field configuration is radially symmetric.
- up to a global rotation of  $S^2$ , the solution “lives” in the  $\phi_1, \phi_3$  plane of the target space ( $S^2$ ).

To study this field configuration further we make the following ansatz:

$$\phi = (\sin f(r, t), 0, \cos f(r, t)). \quad (23)$$

The lagrangian density then becomes

$$L = \pi \int dr r (\partial_t f \partial_t f - \partial_r f \partial_r f - \mu^2 (1 - \cos(f))). \quad (24)$$

and the equation reduces to the radial sine-Gordon equation:

$$f_{tt} - f_{rr} - \frac{f_r}{r} + \mu^2 \sin(f) = 0. \quad (25)$$

This equation has already been studied in [9], where it was shown that it has time dependent solutions similar to a breather, but which radiate their energy and slowly die out. The authors of [9] decided to call such configurations pulsions.

In [10] we have also shown that there exist stable time dependent solutions. The radial field configurations of (25) radiate relatively quickly when their amplitude of oscillation is relatively small, that is when the value of  $f$  never becomes larger than  $\pi/2$  at the origin (these are the pulsions studied in [9].) When the amplitude of oscillation is larger than  $\pi/2$  the configuration radiates its energy very slowly and asymptotically reduces the amplitude of oscillation to  $\pi/2$  with a period of oscillation  $T \sim 20.5$  (when  $\mu^2 = 0.1$ ). We have decided to call this asymptotic configuration pseudo-breather. The time dependant solutions with amplitude larger than  $\pi/2$  can then be considered as excited pseudo-breathers. By trial and error we have found that

$$\begin{aligned} f(r, 0) &= 4 \operatorname{atan} \left( C \exp \left( -\frac{2}{\pi} \frac{\mu r}{K} \operatorname{atan} \left( \frac{\mu r}{K} \right) \right) \right) \\ \frac{\partial f}{\partial t}(r, 0) &= 0 \end{aligned} \quad (26)$$

with  $K = 10$  and  $C = \tan(\pi/8)$  is a good initial condition for this metastable pseudo-breather solution.

Our numerical study of the pseudo-breather shows that it is metastable; even a small perturbation is sufficient to reduce its amplitude of oscillation and transform it into a pulsion. On the other hand, the excited pseudo-breathers are relatively stable: the larger the excitation energy, the larger the perturbation needed to transform them into a pulsion.

As in the case of plane wave solutions we have to check that once they are imbedded into  $S^2$  they are still stable. We have indeed checked this numerically and we have found that the solution described by (23) and (25) is indeed stable in the  $S^2$  model.

The energy of this new breather-like solution is given by

$$E_{PB} \sim 3.97$$

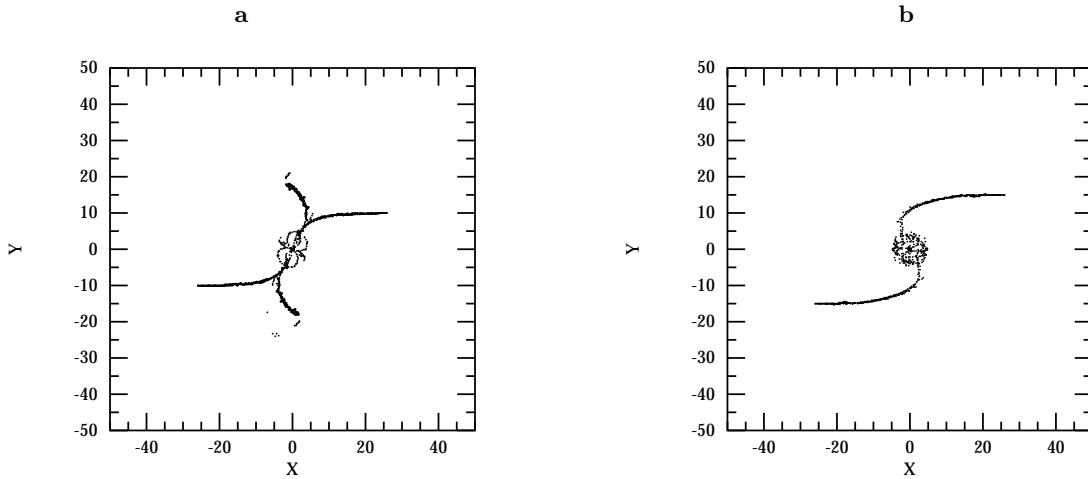


**Fig. 8. a:** Pseudo-Breather scattering trajectory. Impact Parameter: 10,  $v = 0.2$  **b:** Pseudo-Breather scattering trajectory. Impact Parameter: 15,  $v = 0.2$

which means that it is 2.5 heavier than the baby-Skyrmion. Moreover, its topological charge density is identically zero but it has enough energy to decay into a Skyrmion anti-Skyrmion pair. In what follows we shall refer to these field configurations as pseudo-breathers.

In practice, it is very difficult to have a field configuration of a pseudo-breather. However, we can find approximate field configurations which still radiate energy and asymptotically reach the stable (or perhaps only metastable) configuration of the pseudo-breather. The excess of energy over the final configuration can then be seen as an excitation energy which is slowly radiated away. During any scattering process solitons tend to exchange or radiate some energy. When the excitation energy is large enough, the outgoing pseudo-breather-like configuration may have enough energy to evolve into the stable pseudo-breather field; otherwise, it ends up with less energy than the metastable configuration and progressively dies out.

The scattering properties of pseudo-breathers are quite interesting. When the pseudo-breathers are imbedded into the baby-Skyrmion model the field configurations have an extra degree of freedom corresponding to their orientation inside the  $\phi_1, \phi_2$  plane. When two pseudo-breathers are set at rest near each other, the force between them depends very much on their relative orientation: when they are parallel to each other and oscillate in phase, they attract each other, overlap and form a new structure which appears to be an excited pseudo-breather. This pseudo-breather then slowly radiates away its energy. The non-topological nature of pseudo-breathers means that they can indeed merge to form a new structure of the same type.

If the two pseudo-breathers are anti parallel, *i.e.* if they oscillate completely out of phase, then the force between them is repulsive. When the two pseudo-breathers have a different orientation they slowly rotate themselves until they become parallel; then they move towards each other and form an excited pseudo-breather structure.

When two pseudo-breathers are sent towards each other with some kinetic energy, the scattering becomes more involved. Depending on the initial speed or the scattering impact parameter, they either merge into a single pseudo-breather or they undergo a forward scattering. The details of these scattering properties are given in [10]. In Fig. 8 we show two trajectories corresponding to the position of the local maxima of the energy density seen in two simulations. The arrows indicate the direction of movement. When the two pseudo-breathers overlap, their energy density exhibits quite a few local maxima, hence the circles observed at the centers of both pictures. For both scatterings the initial speed was 0.2, the only difference between them was in the values of the initial impact parameter.

## 9 Pseudo-Breather-Skyrmion scattering

As we have seen, the baby-Skyrmion model has two different types of extended solutions. The Skyrmions are topological solitons which are very stable, while the pseudo-breathers are time-periodic solitons which can slowly decay if they are perturbed too much. It is very unusual to have a model that exhibits two such different stationary structures and so it is interesting to analyse how they interact with each other.

When a Skyrmion and a pseudo-breather are put at rest next to each other the overall interaction between them makes the Skyrmion slowly move away from the pseudo-breather-like configuration while the pseudo-breather loses some of its energy faster than when it is placed there by itself.

To scatter a Skyrmion with a pseudo-breather we have placed the pseudo-breather soliton at rest, and we have sent the Skyrmion towards it. We have performed this scattering for different orientations of the pseudo-breather, for different values of the impact parameter and for a few different speeds. In each case, the pseudo-breather was initially located at the origin while the Skyrmion always



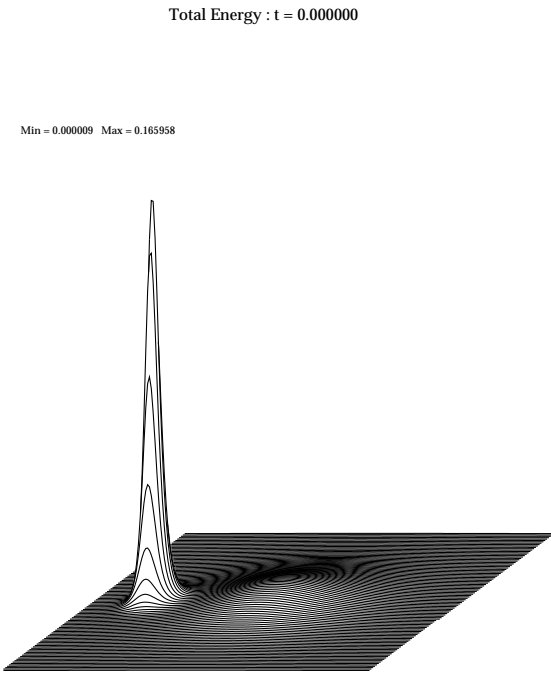


**Fig. 9.** Skyrmion and pseudo-breather at rest

started from  $(x_0, y_0)$  where  $x_0$  is the initial position along the  $x$  axis and  $y_0$  is the impact parameter. The pseudo-breather was oscillating in the  $(\phi_1, \phi_2)$  plane along the direction  $(\cos(\alpha), \sin(\alpha))$ .

In Fig. 9 we show the initial condition corresponding to a baby-Skyrmion next to a pseudo-breather. We note that the Skyrmion is much more spiky than the breather.

Our numerical results are summarised in the following 4 tables.

**Table 1.a.** Impact parameter and speed dependence of the scattering angle ( $\alpha = 0, x_0 = -20$ )

$v \setminus y_0$	15	10	7.5	5	3.5	2.5	1.25
0.2	5	18	31	39	58	67	-108
0.3	6	26	16	15	36	35	-24
0.4	4	7	11	0	-9		-8

**Table 1.b.** Impact parameter and speed dependence of the scattering angle ( $\alpha = \pi/2, x_0 = -20$ )

$v \setminus y_0$	15	10	7.5	5	3.5	2.5	1.25
0.2	8	19	27	30	21	21	90
0.3	6	16	24	23	21	29	23
0.4	5	20	21	20	18	19	4

**Table 1.c.** Impact parameter and speed dependence of the scattering angle ( $\alpha = \pi/4, x_0 = -20$ )

$v \setminus y_0$	15	10	7.5	5	3.5	2.5	1.25
0.2	7	18	29	32	52	62	-166
0.3	7	14	15	2.5	22	45	-27
0.4	3	8	8	15	14	24	-43

**Table 2.** Scattering angle as a function of the initial distance ( $\alpha = \pi/2, y_0 = 2.5$ )

$v \setminus x_0$	15.2	16.2	17.2	18.2	19.2	20.2
0.2	38	33	33	38	31	21
0.4	15	16	17	20	22	19

The amount of energy lost by the pseudo-breather during the scattering is larger when the overlap between the Skyrmion and the breather, both in time and space, increases. In some cases the pseudo-breather is completely destroyed by the collision. The oscillation of the pseudo-breather makes the interaction time dependent, and, as a result, we are unfortunately unable to extract a simple pattern from the tables of the scattering angles.

## 10 Conclusions

We have shown that the baby-Skyrmion model has many interesting classical solutions in addition to the Skyrmion solitons. The first class of solutions describe excited states of Skyrmons and anti-Skyrmions which are unstable with respect to perturbations.

The second class of solutions involves non-topological stationary stationary field configurations which are periodic in time. They are relatively stable but, as they are nontopological in nature, they can be destroyed by sufficiently large perturbations.

*Acknowledgements.* One of the authors (AK) thanks The Department for Mathematical Science of University of Durham for hospitality during his visit. This visit was supported by INTAS grant 93-633 and partly by grants INTAS-CNRS1010-CT93-0023 and RFFR-95-02-04681.

We want to thank R.S. Ward for helpful comments.

## References

1. B.M.A.G. Piette, B.J. Schroers, W.J. Zakrzewski, Nucl. Phys. B **439** (1995) 205
2. B.M.A.G. Piette, B.J. Schroers, W.J. Zakrzewski, Z. Phys. C **65** (1995) 165
3. B.M.A.G. Piette, H.J.W. Muller-Kirsten, D.H. Tchrakian, W.J. Zakrzewski, Phys. Lett. B **320** (1994) 294
4. T.H.R. Skyrme, Proc. Roy. Soc. A260 (1961) 125; G.S. Adkins, C.R. Nappi, E. Witten, Nucl. Phys. B **228** (1983) 552
5. R.A. Leese, M. Peyrard, W.J. Zakrzewski, Nonlinearity **3** (1990) 773
6. M. Peyrard, B. Piette, W.J. Zakrzewski, Nonlinearity **5**, 585 (1992).
7. A. Kudryavtsev, B. Piette, W.J. Zakrzewski, Z. Phys. C **60**, (1993) 731.
8. see e.g. M.J. Ablowitz, P.A. Clarkson – Solitons, Nonlinear Evolution Equations and Inverse Scattering – CUP (1991)
9. P.L. Christiansen, P. Lomdahl, Physica 2D (1981) 482
10. B. Piette, W.J. Zakrzewski, Durham preprint DTP-97/15
11. A. Kudryavtsev, JETP Letters **22**, 82 (1975)
12. J. Geicke, Phys. Scrip. 31 450 (1985)
13. I.L. Bogolyubski, V.G. Machan'kov, JETP Letters **24**, 12 (1976)